

# Operating Deflection Shapes from Strain Measurement Data

Timothy G. Hunter, Ph.D., P.E.  
President  
Wolf Star Technologies, LLC  
3321 N. Newhall St., Milwaukee, WI 53211

## Abstract

Strain gauges are often more advantageous for experimentally analyzing linear dynamic structures due to their lightweight and use for understanding the material response of these structure to external loading. Presented in this paper is an alternative approach to traditional approaches in structural dynamics. The theoretical presentation will describe a practical implementation of a technique using strain data to recover the modal participation factors for linear dynamic analysis.

## Keywords

modal, correlation, strain, FEA, MPF

## Introduction

Presented here is an approach to derive the modal participation factors of a structure directly from strain gauge measurements. Calculation of the response of structures undergoing external excitation can be approximated using the theory of modal superposition. The dynamic responses of flexible structures result in strain on the structure. Strain signals can be measured during the dynamic event. These strains may be projected onto the strains of the individual mode shapes of the structure. The projection of the experimentally measured strains onto the modal strains will result in a scalar indicating the participation of the individual mode in the dynamic response. If this is done for a sufficient number of modes in the structure, then the total response may be reconstructed using modal superposition.

## Theory

The basic theory in dynamic modal analysis is based upon the N-DOF equation of motion [1]:

$$M \ddot{X} + K X = F(t) \quad (1)$$

If the response is assumed to be harmonic, the general form of the response may be written as:

$$X = \psi e^{i\omega t} \quad (2)$$

Expanding this assumption into the equation of motion and solving the homogeneous equation yields the eigenvalue problem:

$$[-M \omega^2 + K] \psi = \{0\} \quad (3)$$

From equation 3,  $\omega$  is the natural frequencies of the structure and  $\psi$  represents the mode shapes.

The particular solution to equation 1 is assumed to be of the form:

$$X(t) = \psi \{z(t)\} \quad (4)$$

The vector of functions,  $z(t)$ , are the scaling functions for each of the mode shapes,  $\psi$ , which satisfy equation 1. Through application of the properties of orthogonality, the spatial 2<sup>nd</sup> order differential equation 1 can be rewritten in modal terms as:

$$\begin{aligned}
\tilde{M} \ddot{z} + \tilde{K} z &= \tilde{F}(t), \text{ where} \\
\tilde{M} &= \psi^T M \psi \text{ (modal mass)} \\
\tilde{K} &= \psi^T K \psi \text{ (modal stiffness)} \\
\tilde{F} &= \psi^T F \psi \text{ (modal force)}
\end{aligned} \tag{5}$$

The properties of equation 5 are such that there are n decoupled 2<sup>nd</sup> order differential equations, where n is the number of mode shapes [1]. The 2<sup>nd</sup> order differential equations can be solved for z(t) using standard closed form techniques or numerical techniques such as Runge-Kutta. The functions, z(t), will be the set of scaling functions for each of the mode shapes. These are commonly known as modal participation functions (MPF). The total response of the structure due to externally applied forces, F(t), is then given by:

$$X(t) = \sum_{i=1}^n \psi_i * z_i(t) \tag{6}$$

### Problem Formulation

The approach presented here will leverage the basic concepts known as influence coefficients [2]. The overall concept comes from the linear mechanics relationship as illustrated below:

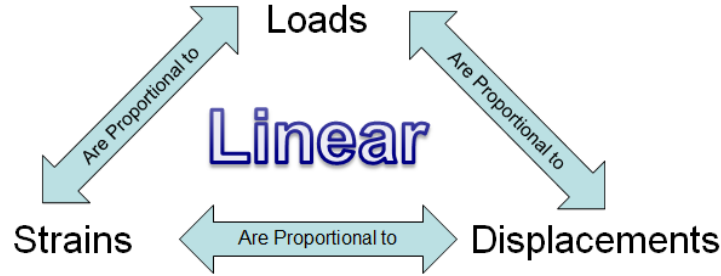


Fig. 1: Linear mechanics relationship

This relationship may be expressed mathematically as:

$$[F] = [K][X] \tag{7}$$

and

$$[\epsilon][C] = [F] \tag{8}$$

In equation 7, the set of displacement vectors [X] represent the deflection due to the set of applied forces. In the special case of dynamics, the applied forces could be the modal inertia loading of the structure. The resulting deflection would be the mode shapes as calculated from equation 3. In standard finite element analysis (FEA), these deflections would be the mode shape results. The FEA solution would also yield the corresponding strain due to the deflection of the mode shapes. Equation 8 implies that there is a unique relationship between each mode shape and the corresponding strain field. The set of mode shapes can be represented as the identity matrix [I] with the size of n modes by n modes. Equation 8 may be rewritten as:

$$[\epsilon][C] = [I] \tag{9}$$

Equation 9 may readily be solved for [C] by:

$$[C] = [\epsilon^T \epsilon]^{-1} \epsilon^T \tag{10}$$

The reader may recognize this as the standard expression for least square fit [3]. A search algorithm is deployed to find a subset of the strain field (e.g. strain gauge locations) that maintain a robust and stable C matrix. The key is to find strain gauge locations that guarantee that the inverse in equation 10 is well defined. This is done by recognizing that an inverse of a matrix can be calculated by dividing the adjoint of the matrix (matrix of cofactors) by the determinant of the matrix [4] as shown in equation 11:

$$A^{-1} = \frac{adj(A)}{|A|} \quad (11)$$

The strain gauges are then found subject to the objective function in equation 12 to ensure the most stable possible expression for the correlation matrix, C.

$$|\varepsilon^T \varepsilon| \rightarrow \max \quad (12)$$

If the strain gauges are laid based upon the strain fields from analytical mode shapes for the structure, it will now be possible to understand the participation of the mode shapes in the overall structural response. This will be done by simply multiplying the strains from test measurements by the correlation matrix extracted from the FEA mode shapes via equation 13.

$$\{\varepsilon_{test}\} * [C] = [F_{MPF}] \quad (13)$$

Expanding equation yields:

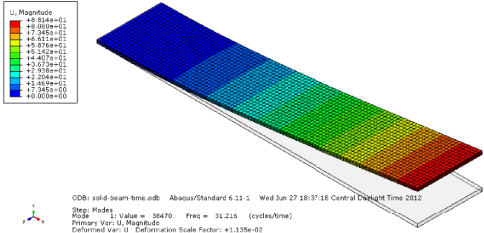
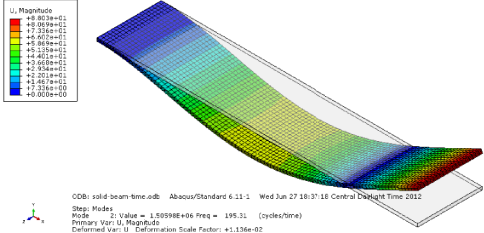
$$\begin{bmatrix} \varepsilon_{t1, g1} & \varepsilon_{t1, g2} & \varepsilon_{t1, g3} & \cdots & \varepsilon_{t1, gm} \\ \varepsilon_{t2, g1} & \varepsilon_{t2, g2} & \varepsilon_{t2, g3} & \cdots & \varepsilon_{t2, gm} \\ \vdots & \vdots & \vdots & \ddots & \vdots \\ \varepsilon_{t_{end}, g1} & \varepsilon_{t_{end}, g2} & \varepsilon_{t_{end}, g3} & \cdots & \varepsilon_{t_{end}, gm} \end{bmatrix} [C] = \begin{pmatrix} F_{t1, mode 1} & F_{t1, mode 2} & \cdots & F_{t1, mode n} \\ F_{t2, mode 1} & F_{t2, mode 2} & \cdots & F_{t2, mode n} \\ \vdots & \vdots & \ddots & \vdots \\ F_{t_{end}, mode 1} & F_{t_{end}, mode 2} & \cdots & F_{t_{end}, mode n} \end{pmatrix} \quad (14)$$

## Case Studies

To test this concept, a fully analytical study will be performed. Two cases are presented. The first case is a cantilever beam under going sinusoidal excitation. The second case will be a prototypical motorcycle headlamp undergoing complex base excitation.

### Cantilever Beam

An aluminum cantilever beam of dimensions 10 inches x 2 inches x 0.1 inches is fixed at one end. The natural frequencies are calculated using Abaqus FEA software. The natural frequencies are compared to hand calculation from Roark [5]. The comparison of natural frequency is shown below:

Mode	Frequency (hz)		Mode shape
	Roark	Abaqus	
1	31.8	31.22	 <p>ODB: solid-beam-time.job; Abaqus/Standard 6.11.1; Wed Jun 27 16:37:18 Central Daylight Time 2012 Step: Modes Mode: 1; Value = 33470; Freq = 31.216 (cycles/time) Primary var: U; Magnitude Deformed var: U; Deformation Scale Factor: +1.135e-02</p>
2	198.6	195.31	 <p>ODB: solid-beam-time.job; Abaqus/Standard 6.11.1; Wed Jun 27 16:37:18 Central Daylight Time 2012 Step: Modes Mode: 2; Value = 1.00998E+04; Freq = 195.31 (cycles/time) Primary var: U; Magnitude Deformed var: U; Deformation Scale Factor: +1.135e-02</p>

Mode	Frequency (hz)		Mode shape
	Roark	Abaqus	
3		319.13	
4	556.9	548.16	
5		616.58	

**Fig. 2: Frequencies, Mode Shapes Cantilever Beam**

Note that the formulas from Roark only calculate the in-plane bending modes. The Roark calculations do not accommodate the out of plane bending or torsion modes of the beam. In this case the 3<sup>rd</sup> and 5<sup>th</sup> modes are out of plane torsion and bending modes.

A series of strain gauge locations are chosen in order to be sensitive to the 5 mode shapes shown in figure 3. Ten strain gauges were chosen in order to provide a robust relationship between strain data and the mode shapes.

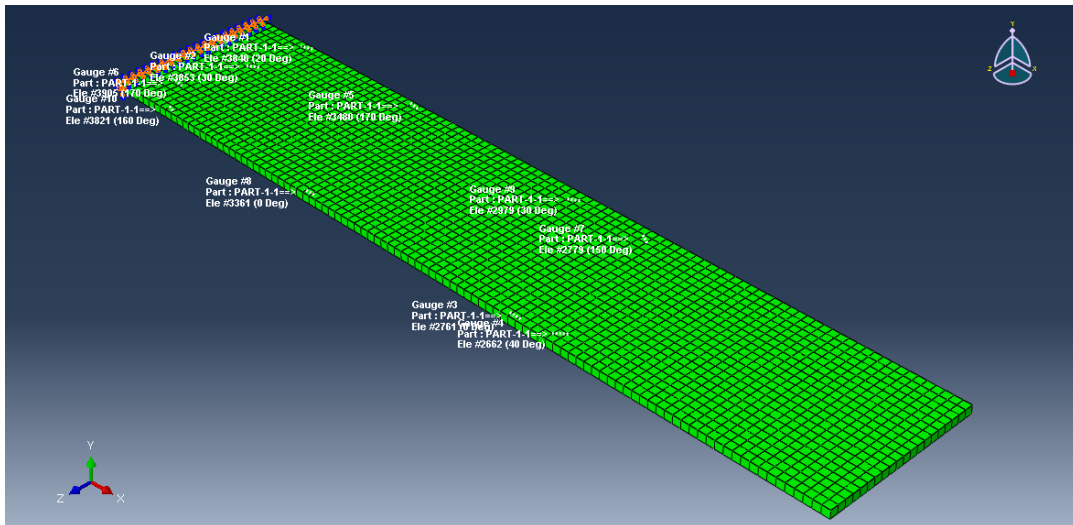


**Fig. 3: Gauge placement, cantilever beam**

The FEA Model was excited by a 35 hz sine wave with the amplitude of 0.1 lbf. The point of excitation is the center of the free end of the beam as shown in figure 4.

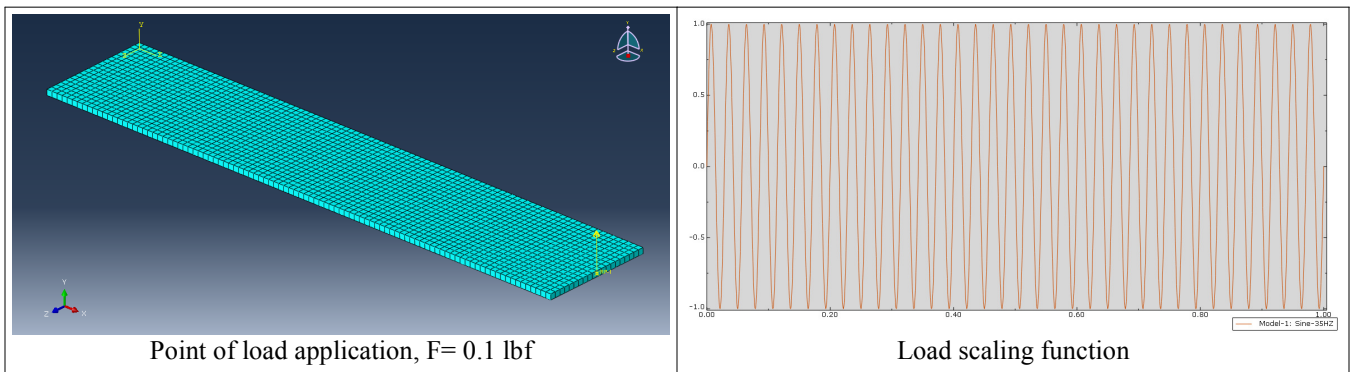


**Fig. 4: Load and forcing function for cantilever beam**

The strain data was collected at the indicated strain gauge locations. These strains were then projected onto the correlation matrix,  $[C]$ . The resulting participation functions are plotted along with the calculated modal participation functions from the FEA modal response analysis. These theoretical and experimentally calculated from strain MPFs are shown in figure 5. The red curves are the modal participation functions from the Abaqus FEA analysis. The curves represented by hollow blue circles are the modal participation functions calculated from the strain data. There is excellent correlation for all modes except modes 3 and 5. Looking at the MPF factors for modes 3 and 5, they have an overall magnitude on the order of  $1E-15$ . This is well beyond the precision of the strain data provided for the reconstruction of the MPF signals.

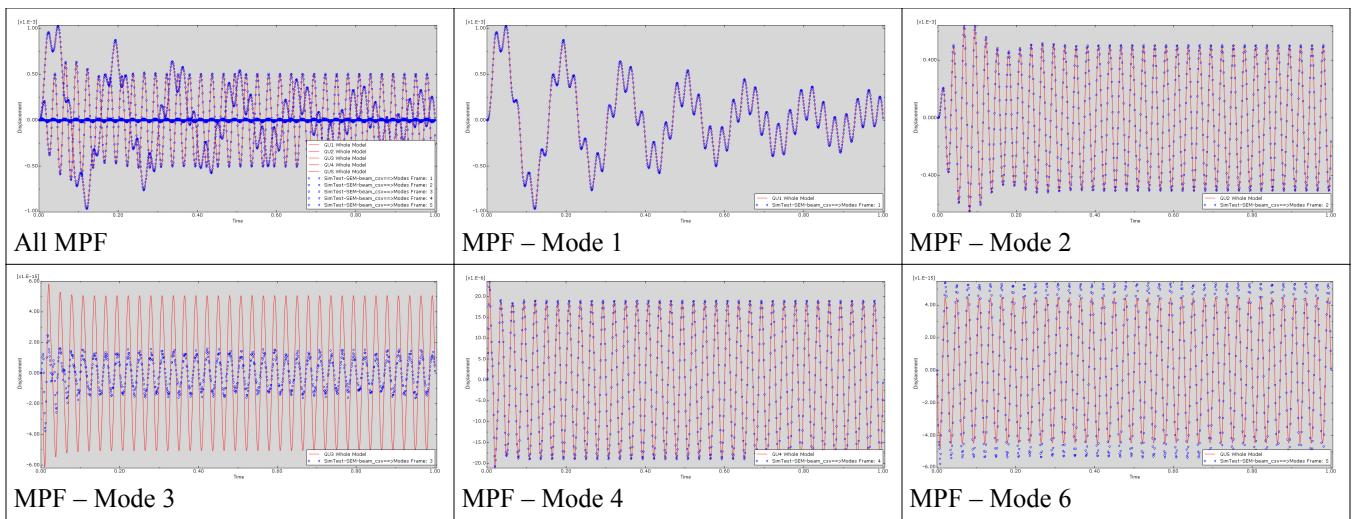


**Fig. 5: Modal participation factors, FEA and Strain based**

These modal participation functions were used to reconstruct the strain at the gauge locations for another method of correlation. Figure 6 shows the strain plots resulting from the linear superposition. The green curves represent the “measured” strain signal from the forced response FEA analysis. The blue curves represent the reconstructed strain response using the experimentally created loading modal participation functions. These curves are line on line with zero percent error between the “measured” strain data and the simulated strain data from the reconstructed MPFs.

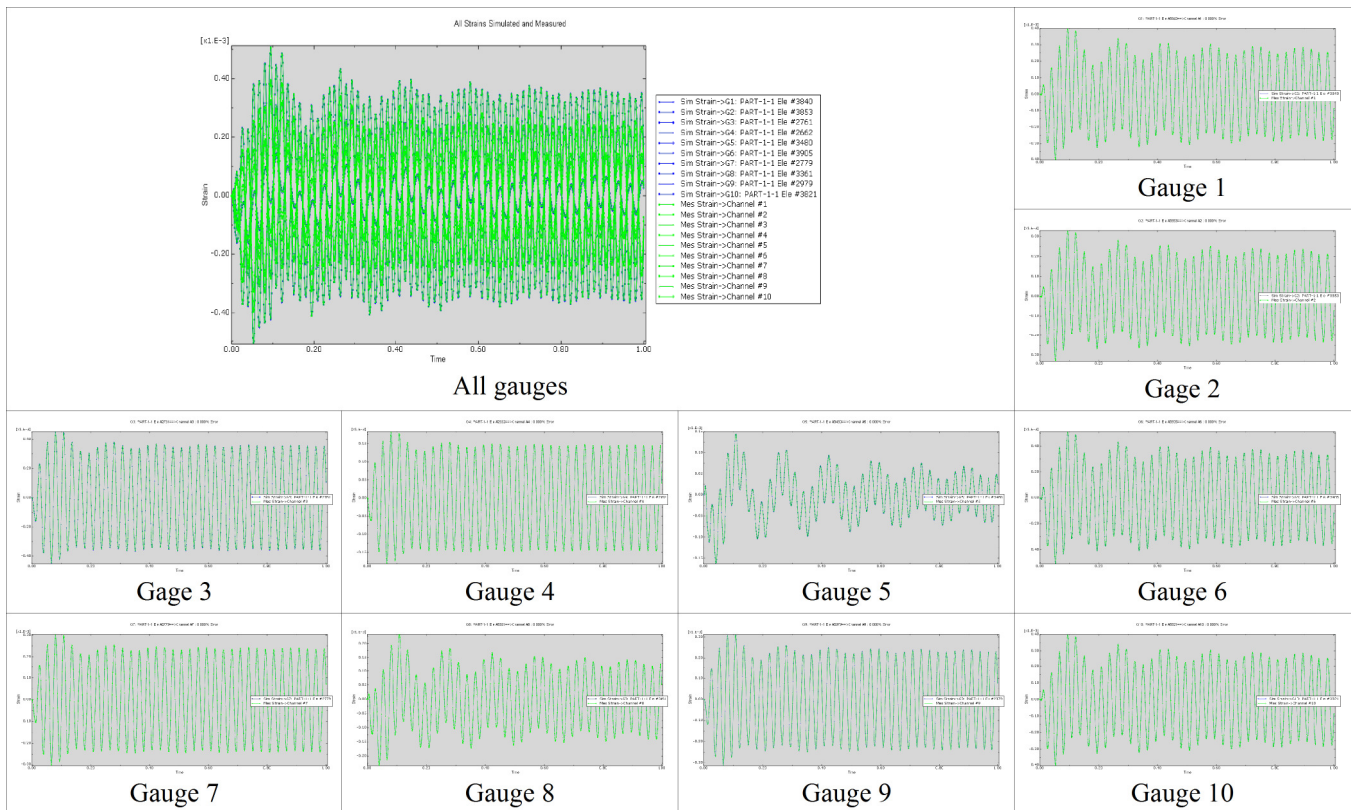


**Fig. 6: Strain correlation, cantilever beam**

## Prototypical Motorcycle Headlamp

Similar to the cantilever beam case study, the headlamp being modeled here will be solved for 5 modes. Strain gauges will be placed in such a fashion as to robustly capture the modal response. The mode shapes are shown in figure 7. The strain gauge placement is shown in figure 8.

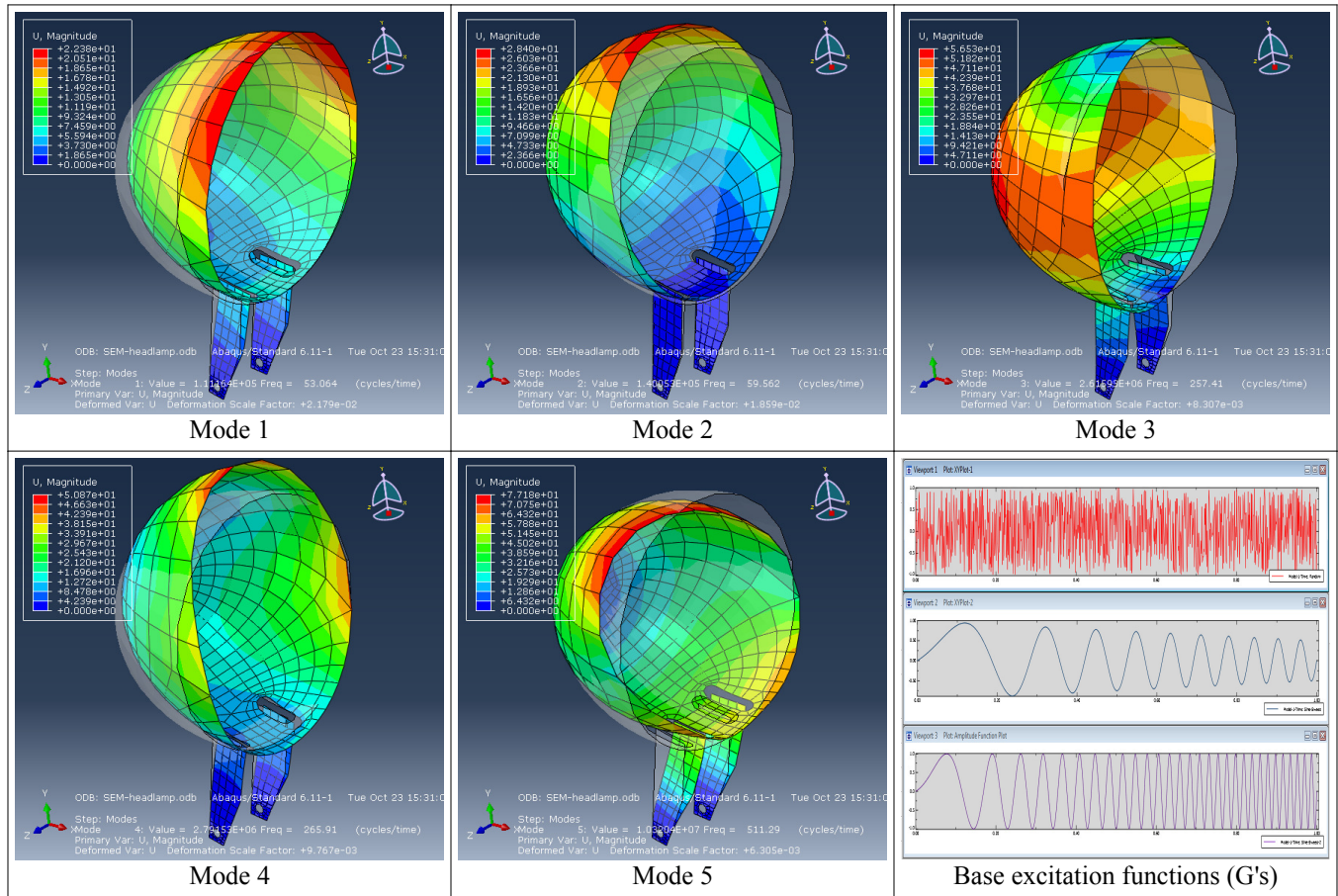


**Fig. 7: Headlamp mode shapes and base excitation functions**

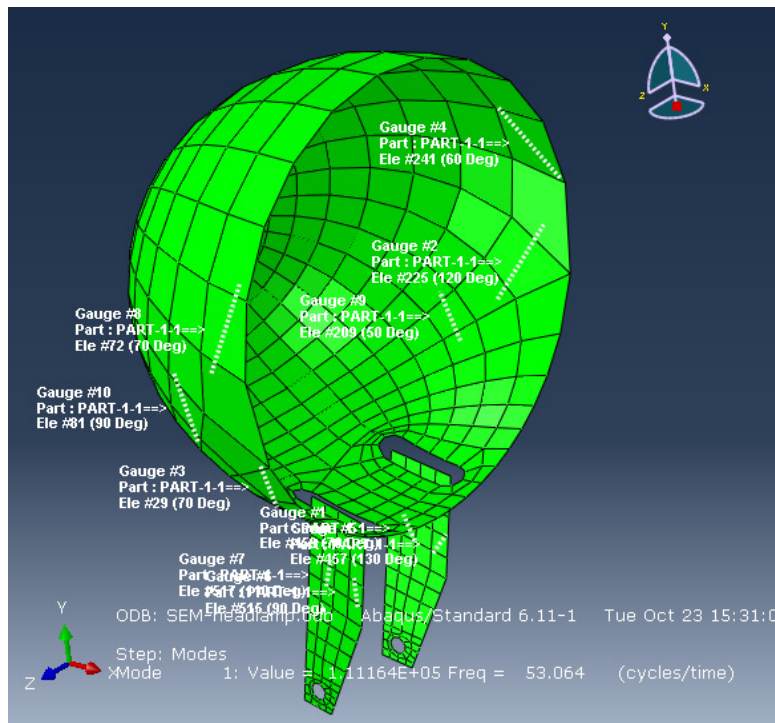


**Fig. 8: Strain Gauge Placement, headlamp**

A set of strain signals was generated at the strain gauge locations shown in figure 8. The strain signals are the result of the base excitation by the forcing functions shown in figure 7. These strain signals will simulate a test data collection of the headlamp structure in operation. These strain signals were then used to re-construct the modal participation functions. The comparison of the analytical modal participation functions from FEA to the modal participation functions calculated from the strain signals. The MPF signals from FEA are plotted in red, and the MPF signals calculated from strain are shown as blue hollow circles in figure 9.

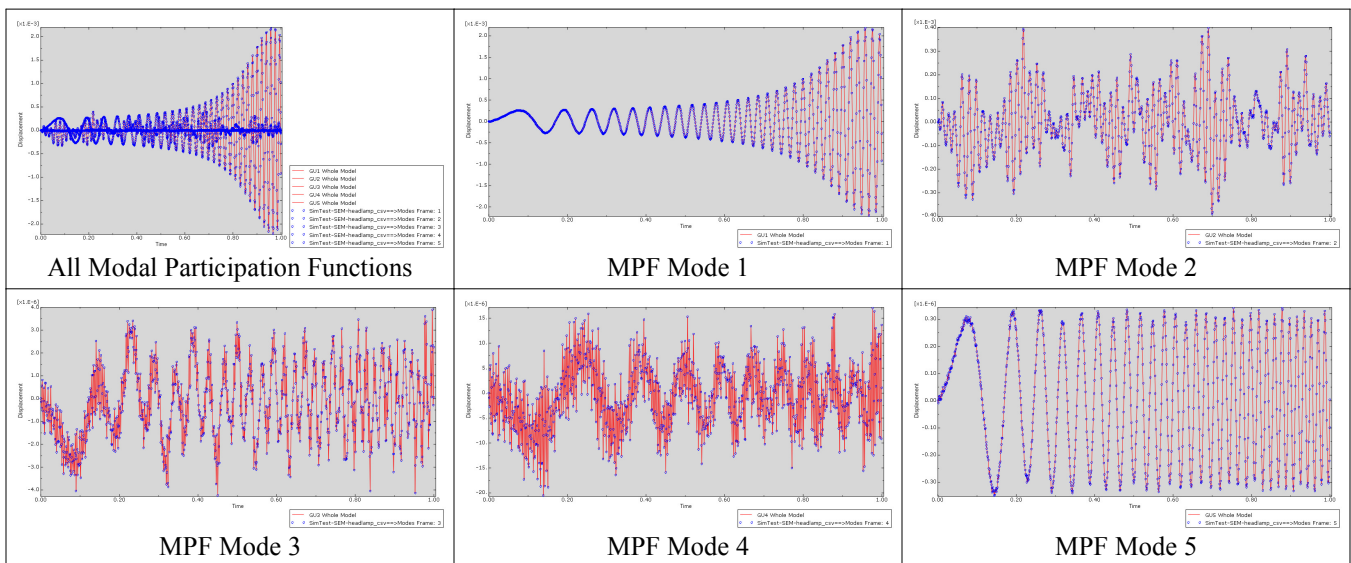


**Fig. 9: Modal participation factors, FEA and Strain based**

The strain “measured” strain signals are plotted with the reconstructed strain signals from the MPF functions calculated from the strain data. These are shown in figure 10. The original strain signals are shown in green and the reconstructed strain

signals are shown in blue. Again, as in the case of the cantilever beam, the error between the “measured” strain data and the simulated strain data from the reconstructed MPFs is zero.

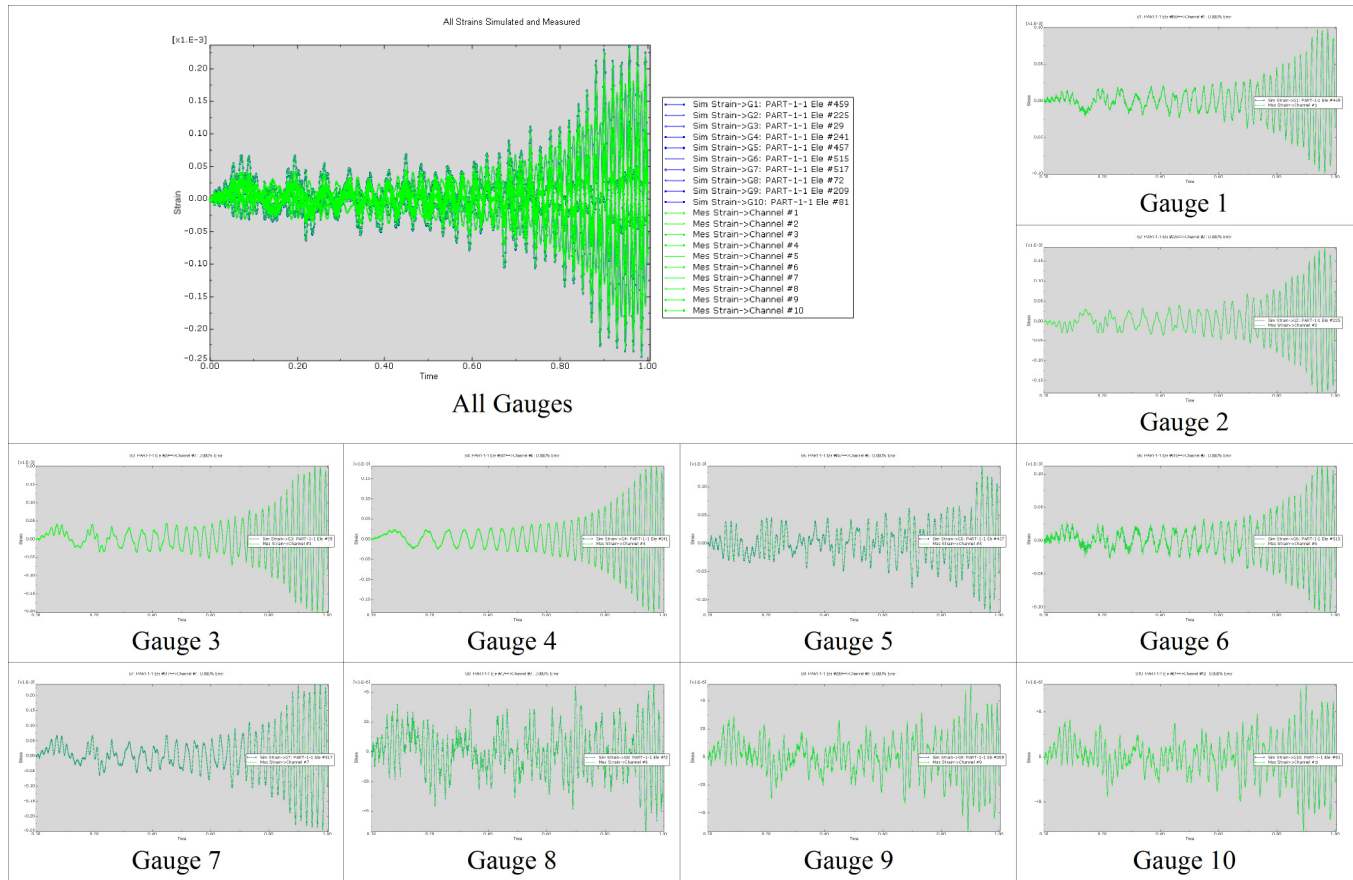


**Fig. 10: Strain correlation, headlamp**

## Conclusions / Discussion

Presented here is a practical approach for understanding dynamic displacement based upon strain gauge data. This technique has the advantage of working with light weight strain gauges. In addition, strain gauges are working directly with displacement domain data and can very accurately capture the flexural response of the structure. An additional advantage of the technique is that it can be combined with quasi-static loading. If the quasi-static loading includes unit perturbations of the connection degrees of freedom (DOF), then resulting MPF reconstruction will essentially be a Craig-Bampton response analysis.

## References

- 1) Thomson, William Tyrrell. *Theory of Vibration with Applications*. Englewood Cliffs, NJ: Prentice-Hall, 1981. Print.
- 2) Rao, S. S. "6.3 Influence Coefficients." *Mechanical Vibrations*. Upper Saddle River, NJ: Pearson Prentice Hall, 2004. 455-57. Print.
- 3) Kwak, Jin Ho, and Sungpyo Hong. *Linear Algebra*. Boston: Birkhäuser, 1997. Print.
- 4) Berberian, Sterling K. *Linear Algebra*. Oxford: Oxford UP, 1992. Print
- 5) Roark, Raymond Jefferson., and Warren C. Young. "Table 36 - Natural Frequencies of Vibration for Continuous Members." *Roark's Formulas for Stress and Strain*. New York [u.a.: McGraw-Hill, 1989. 714-15. Print.